Hydrol. Earth Syst. Sci. Discuss., 5, 2409–2423, 2008
www.hydrol-earth-syst-sci-discuss.net/5/2409/2008/

Hydrology and Earth System Sciences Discussions

Thermal conductivity of unsaturated clay-rocks

D. Jougnot[1,2,3] **and A. Revil**[1,3]

[1]Colorado School of Mines, Green Center, Department of Geophysics, Golden, CO, USA
[2]ANDRA, Chatenay-Malabry, France
[3]CNRS-LGIT (UMR 5559), University of Savoie, Equipe Volcan, Le Bourget-du-Lac, France

Received: 4 August 2008 – Accepted: 8 August 2008 – Published: 28 August 2008

Correspondence to: A. Revil (arevil@mines.edu)

Published by Copernicus Publications on behalf of the European Geosciences Union.

Abstract

The thermal conductivity of porous materials can be related to the electrical conductivity and therefore electrical resistivity tomography can be used to map the thermal conductivity of porous rocks. In this paper, a relationship is developed to connect the thermal conductivity of unsaturated clay-rocks to the thermal conductivity of the different phases of the porous composite, a textural parameter called the thermal formation factor, and the tortuosity of the water phase. The thermal formation factor is related to the electrical formation factor and to the first Archie's first exponent m. The tortuosity of the water phase is related to the second Archie's exponent n and to the relative saturation of the water phase. A very good agreement is obtained between the new model and thermal conductivity measurements of packs of glass beads and cores of the Callovo-Oxfordian argillite at different saturations of the water phase. Anisotropy of the effective thermal conductivity is mainly due to the anisotropy of the thermal conductivity of the solid phase.

1 Introduction

The modelling of the thermal conductivity of unsaturated clay-rich materials has applications to the characterization of the thermal anomalies associated with oil and gas reservoirs (Revil, 2000), climate change (Kooi, 2008), and to study the transport properties of deep argillaceous formation under investigation to potentially host nuclear wastes (Giraud et al., 2007).

In the context of the storage of nuclear waste in deep argillaceous formations, the knowledge of thermal conductivity of these formations is of prime importance to study their behaviour in response to temperature variations. The possibility to connect thermal conductivity to parameters that can be imaged through geophysical methods (like the electrical conductivity and the dielectric constant) offers a way to image non-intrusively, using electrical resistivity tomography and georadar, this key-parameter using a hydrogeophysical synthetic model generators for instance (e.g., Giroux and Chouteau, 2008).

Several methods have been developed in the last decades to estimate the effective thermal conductivity of unsaturated porous rocks (e.g., Woodside and Messmer, 1961; Cosenza et al., 2003; Kohout et al., 2004, Gruescu et al., 2007; and Giraud et al., 2007; just to cite few examples). However, these models do not establish a clear relationship between electrical (or dielectric) parameters, like the electrical formation factor, and the effective thermal conductivity of the porous material.

Revil (2000) developed a model that relates directly the thermal conductivity of a porous material to the electrical formation factor arising in the electrical conductivity and dielectric problems. In the present work, we extend and test the model of Revil (2000) to unsaturated conditions for the Callovo-Oxfordian argillite of the Paris basin (in France).

2 Proposed model

Using a differential effective medium approach, Revil (2000) developed the following closed-form relationship for the effective thermal conductivity λ of a fluid saturated porous material:

$$\lambda = \frac{\lambda_f}{f}\left[f\Theta + \frac{1}{2}(1-\Theta)\left(1-\Theta+\sqrt{(1-\Theta)^2+4f\Theta}\right)\right]. \tag{1}$$

where $\Theta \equiv \lambda_s/\lambda_f$ (λ_s and λ_f are the thermal conductivities of the solid and fluid phases, respectively) and f is the "thermal formation factor" defined by:

$$f = \phi^{\frac{m}{1-m}}, \tag{2}$$

where ϕ is the porosity, m is the Archie's first exponent (also called the cementation exponent) ranging typically between 1.3 (for unconsolidated sands) to 2.0 (for consolidated rocks) (see Archie, 1942; and Lesmes and Fiedman, 2005). If the medium is anisotropic, f λ_s are second order (symmetric) tensors. The exponent m is defined by the first Archie law $F = \phi^{-m}$ where F is the electrical formation factor (e.g., Archie, 1942; Lesmes and Friedman, 2005). The electrical formation factor is also defined as the ratio between the tortuosity of the pore space α to the connected porosity: $F = \alpha/\phi$. The two formation factors are related by $f = F^{1/(m-1)}$ (Revil, 2000).

In unsaturated conditions, two fluids (brine, subscript w, and air, subscript a) are present in the pore space of the medium. Following Linde et al. (2006) and Revil et al. (2007) for the conductivity and dielectric constants of unsaturated sandstones, we can relate the thermal conductivity of the fluid phase to the saturations of the brine s_w and to the saturation of air $(1-s_w)$ by using a generalized second Archie law:

$$\lambda_f = s_w^n \lambda_w + \left(1 - s_w^n\right) \lambda_a, \quad (3)$$

where λ_w and λ_a are the thermal conductivities of the brine and air, respectively,n is the second Archie exponent ($n \approx 2.0 \pm 0.5$; Archie, 1942). This exponent describes the evolution of the water phase tortuosity α_w ($\geq \alpha$) with the saturation s_w.

Equations (1)–(3) can be used to determine the effective thermal conductivity of a porous material from the saturation of the water phase while the composition of the solid phase can be used to determine the effective thermal conductivity of the solid, λ_s using the mixture approach. In order to test the previous model, we first present a comparison between this model and the data from Kohout et al. (2004) (see Fig. 1). The data have been obtained using a pack of glass beads (the beads have a mean diameter d=200 μm), ϕ=0.39, λ_s=0.80 W K^{-1} m^{-1}, λ_w=0.61 W K^{-1} m^{-1}, and λ_a=0.02 W K^{-1} m^{-1}. The two exponent m and n are optimized using the Simplex algorithm in a Matlab® routine. Our cost function to minimize is the sum of square residuals (SS_R) between the N experimental observed data y_i and N calculated one y_i':

$$SS_R = \sum_{i=1}^{N} \left(y_i - y_i'\right)^2. \quad (4)$$

HESSD
5, 2409–2423, 2008

D. Jougnot and A. Revil

We use below a normalised sum of square residuals $R_N = SS_R/N$ for making comparison between experiments with different size of data sets. The best fit is obtain with $m=1.70$ and $n=1.52$, which yields $R_N=4.4\times10^{-3}$ (Fig. 1). The value of m agrees with the values of $m=1.7$ determined numerically by Schwartz and Kimminau (1987).

3 Thermal conductivity of the COx argillites

We apply now our model to the Callovo-Oxfordian (COx) argillite samples collected at Bure (in the Eastern part of the Paris basin (Meuse/Haute-Marne, France), at a depth interval ranging from 450 to 525 m. This area has been selected by the French Agency for Management of Radioactive Waste (ANDRA) to study the feasibility of long-term underground storage of radioactive wastes (ANDRA, 2005) (see http://www.andra.fr). The solid matrix of these COx argillites is composed of clays, silica, and calcite and different geologic units have been defined for the COx formation (denoted C2d, C2c, C2b2, C2b1, and C2a). The C2b unit regroups C2b1 and C2b2. In this unit, the clay matrix forms a porous skeleton completely connected. At the micro-scale, this material presents a granular texture. The Cox argillite exhibits different scales of porosity (Fig. 2). The total porosity is equal to $\phi_T=0.18\pm0.01$ in the C2b unit. A fraction of the connected meso-porosity and all the micro-porosity (corresponding to a pore scale <10 nm) contain bound water corresponding to a porosity $\phi_B=0.07$ (therefore $\phi_B=0.39\phi_T$ in the C2b2 unit) (see ANDRA, 2005).

Different methods can be used to probe the porosity of argillite. These methods provide complementary information. For example, Hg porosity is unable to investigate pore size below 4 nm and therefore provides only a lower bound for the total porosity. Calculations based on volumetric weights with a pycnometer provides an upper bound on the total porosity. We will used below this calculated porosity because it is likely to be close to the real porosity because of the small amount of unconnected porosity.

Homand (1998) and Gruescu et al. (2007) performed thermal conductivity measurements of seven argillite core samples from the EST-104 borehole at Bure. These samples belong to the following units: C2c, C2b2, C2b1, and C2a. For each sample, the effective thermal conductivity of the core is measured at various relative water saturation in the range 0 (dry) to 1 (saturated). The dry samples were obtained after heating the samples during 48 h at 105°C. Progressive saturation is then performed at confined and controlled atmosphere. However, the heating treatment required to get away the water phase, could damage the texture of the medium by creating small cracks. A similar process arises during dessication of the water walls of galleries at Bure. Note that there is no intermediate saturations investigated in the range $0<s_w<0.4$ because this range corresponds likely to the bound water porosity ϕ_B.

Homand (1998) demonstrates also the anisotropy of the thermal conductivity of the COx argillite by performing measurement along the axes relative to the stratification (parallel, perpendicular, and at 45°). We discuss first the measurements parallel to the stratification parallel. Our model only needs the following input parameters: λ_s, m, and n (we have λ_a=0.0255 W K^{-1} m^{-1} and λ_w=0.5984 W K^{-1}m^{-1}, see Clauser and Huenges, 1995). We used calculated porosity from Homand et al. (1998). The solid phase thermal conductivity λ_s and the Archie exponents m and n are optimized using the Simplex algorithm combined with a Monte Carlo method by generating 100 a priori values and by taking the median of the Simplex algorithm results for each parameters. The thermal formation factor f is determined from Eq. (2) with the values of ϕ and m. An a priro value of m was provided by Revil et al. (2005) (m=1.95±0.04 for undisturbed water-saturated Cox argilite).

The optimised parameters are reported in Table 1 and allow a good fit of the data (see Fig. 3) (the mean of R_N for the 7 samples is 3.1×10^{-3}). The range of the optimized parameters is very narrow (Table 1): $m \in(1.37;\ 1.54)$, $n \in(1.99;\ 2.16)$, and $\lambda_s \in(2.08;\ 3.04)$ W K^{-1} m^{-1}. We note that the values of m is quite low in regards to the value reported by Revil et al. (2005). The presence of microcracks due to heating is responsible for a decrease of the tortuosity of the pore space and therefore a decrease of the first Archie exponent. The extension of the model of Revil (2000) to unsaturated condition fits very well the experimental data.

HESSD

5, 2409–2423, 2008

In order to test further our model, we performed two additional tests. First, we fix m by taking the value of Revil et al. (2005) (m=1.95) and we optimize only n and λ_s with the Simplex combined with a Monte-Carlo method. We observe that R_N increase by 2 orders of magnitude (the range of the values of n becomes wider: $n \in (1.57; 2.26)$ and λ_s increases $\lambda_s \in (2.78; 3.96)$ W K^{-1} m^{-1}. The choice of m=1.95 is therefore not a good choice for the damaged argillite samples. Then, we performed a second test by taking n=2 and we optimize m and λ_s. We observe no important changes between these results and those had been obtained abobe by optimizing the three parameters m, n, and λ_s (the mean of R_N is 3.2×10^{-3}, $m \in (1.37; 1.54)$ and $\lambda_s \in (2.08; 3.07)$ W K^{-1} m^{-1}). Therefore, the value of n=2 is a good default value.

We have characterized λ_s from some analysis on COx composition of each sample (from Gruescu et al., 2007). We observe a quite good correlation between the quartz fraction χ_{Qz} and the thermal conductivity of the solid phase. The best fit of the data yields λ_s: $\lambda_s=11.0\chi_{Qz}-0.99$ ($R_N=3.19\times10^{-2}$, except for EST2538, Figure not shown). We tried several classical averaging methods to determine λ_s from the mineralogy but none was better than the previous fit.

We also investigated the data reported by Homand (1998) for the direction perpendicular to the stratification (not shown here). In order to quantify the anisotropy of the argilite, we estimate the following mean ratio for the seven samples: $m_{(//)}/m_{(+)}=0.926\pm0.115$, $n_{(//)}/n_{(+)}=1.015\pm0.106$, and $\lambda_{s(//)}/\lambda_{s(+)}=1.265\pm0.320$ where the subscripts (//) and (+) corresponds to the parameter inverted for the data parallel and perpendicular with respect to the stratification, respectively. We observed no strong anisotropy for n, a small anisotropy for m, but clearly a strong anisotropy for λ_s (see Fig. 4). The anisotropy of the solid phase is therefore due to the fabric of the grains with preferential orientations in the plane of stratification.

4 Conclusions

The thermal conductivity model proposed by Revil (2000) has been extended to unsaturated conditions. The advantage of this model is to connect the effective thermal conductivity to the electrical Archie exponents m and n. It seems that $n=2$ could be used to interpret electrical resistivity data (or georadar data) of damaged argilites in terms of thermal conductivity distribution. We may suppose that in undisturbed COx argillites $m=2$ ($\sim$1.95) could be used. Therefore, we believe that it is possible to image non-intrusively the thermal conductivity of the formation using these methods. This will be the purpose of a future work.

Acknowledgements. This work is supported by the CNRS, the French National Agency for Radioactive Waste Management (ANDRA) (S. Altmann and D. Coelho) and GDR-FORPRO (J. Lancelot). The Ph.D. Thesis of D. Jougnot is supported by ANDRA. This is a contribution FORPRO 2007/XX.

CENTRE NATIONAL DE LA RECHERCHE SCIENTIFIQUE

The publication of this article is financed by CNRS-INSU.

References

ANDRA: Dossier 2005: référentiel du site de Meuse/Haute-Marne, Rep. C.RP.ADS.04.0022, ANDRA, Châtenay-Malabry, France, 2005.

Archie, G. E.: The electrical resistivity log as an aid in determining some reservoir characteristics, T. Am. I. Min. Met. Eng., 146, 54–62, 1942.

Clauser, C. and Huenges, E.: Thermal conductivity of rocks and minerals, in: Rocks physics and phase relations: a handbook of physical constants, AGU Reference Shelf 3, edited by: Ahrens, T., American Geophysical Union, Washington, DC, USA, 105–126, 1995.

Cosenza, P., Guérin, R., and Tabbagh, A.: Relationship between thermal conductivity and water content of soils using numerical modelling, Eur. J. Soil Sci., 54(3), 581–588, 2003.
Giraud A., Gruescu, C., Do, D. P., Homand, F., and Kondo, D.: Effective thermal conductivity of transversely isotropic media with arbitrary oriented ellipsoïdal inhomogeneities, Int. J. Solids Struct., 44(9), 2627–2647, 2007.
Giroux, B. and Chouteau, M.: A hydrogeophysical synthetic model generator, Comput. Geosci., 34(9), 1080–1092, 2008.
Gruescu, I. C., Giraud, A., Homand, F., Kondo, D., and Do, D. P.: Effective thermal conductivity of partially saturated rocks, Int. J. Solids Struct., 44, 811–833, doi:10.1016/j.ijsolstr, 2006.
Homand, F.: Mesures thermiques sur le site est, Technical Report ANDRA, DRP0ENG 98-009/A, INPL-LAEGO, France, 1998.
Kohout, M., Collier, A. P., and Štepánek, F.: Effective thermal conductivity of wet particle assemblies, Int. J. Heat Mass Tran., 47, 5565–5574, 2004.
Kooi, H.: Spatial variability in subsurface warming over the last three decades; insight from repeated borehole temperature measurements in the Netherlands, Earth Planet. Sc. Lett., 270(1–2), 86–94, 2008.
Lesmes, D. P. and Friedman, S.: Relationships between the electrical and hydrogeological properties of rocks and soils, in: Hydrogeophysics, edited by: Rubin, Y. and Hubbard, S., Springer, New York, USA, 87–128, 2005.
Linde, N., Binley, A., Tryggvason, A., Pedersen, L. B., and Revil, A.: Improved hydrogeophysical characterization using joint inversion of cross-hole electrical resistance and ground penetrating radar traveltime data, Water Resour. Res., 42, W12404, doi:10.1029/2006WR005131, 2006.
Revil, A.: Thermal conductivity of unconsolidated sediments with geophysical applications, J. Geophys. Res., 105(B7), 16 749–16 768, 2000.
Revil A., Leroy, P., and Titov, K.: Characterization of transport properties of argillaceous sediments. Application to the Callovo-Oxfordian Argillite, J. Geophys. Res., 110, B06202, doi:10.1029/2004JB003442, 2005.
Revil A., Linde, N., Cerepi, A., Jougnot, D., Matthäi, S., and Finsterle, S.: Electrokinetic coupling in unsaturated porous media, J. Colloid Interf. Sci., 313, 315–327, doi:10.1016/j.jcis.2007.03.037, 2007.
Schwartz, L .M. and Kimminau, S.: Analysis of electrical conduction in the grain consolidated model, Geophysics, 52, 1402–1411, 1987.

Woodside, W., and Messmer, J. H.: Thermal conductivity of porous media, I. Unconsolidated sands, J. Appl. Phys., 32, 1688–1699, 1961.

HESSD

5, 2409–2423, 2008

Table 1. Optimized parameters for seven COx argillite samples (porosity corresponding to the calculated porosity from Homand, 1998).

Sample	Geological unit	ϕ (–)	m (–)	n (–)	λ_s (W K^{-1} m^{-1})	R_N (–)
EST 2171	C2c	0.13	1.45±0.01	2.09±0.52	2.38±0.01	3.8×10^{-3}
EST 2186	C2c	0.16	1.37±0.06	2.04±0.51	2.35±0.06	4.3×10^{-3}
EST 2316	C2b2	0.15	1.37±0.01	2.05±0.46	2.16±0.06	1.9×10^{-3}
EST 2326	C2b1	0.17	1.42±0.01	2.02±0.49	2.24±0.01	4.9×10^{-3}
EST 2423	C2b1	0.17	1.38±0.01	1.99±0.35	2.08±0.02	2.1×10^{-3}
EST 2538	C2b1	0.08	1.54±0.09	2.11±0.52	2.41±0.01	2.0×10^{-3}
EST 2566	C2a	0.11	1.42±0.39	2.16±0.53	3.04±0.25	2.8×10^{-3}

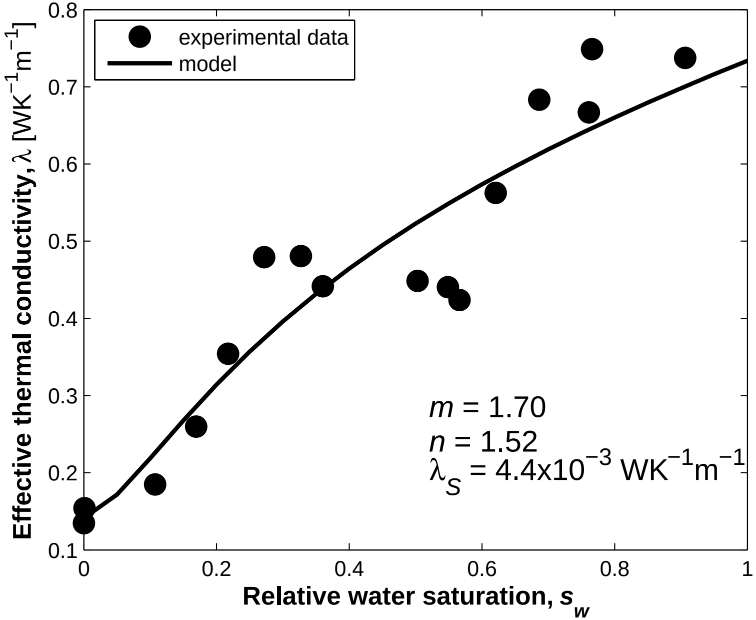

Fig. 1. Fitting proposed model to experimental thermal conductivity measurements of randomly compacted glass beads (data from Kohout et al., 2004).

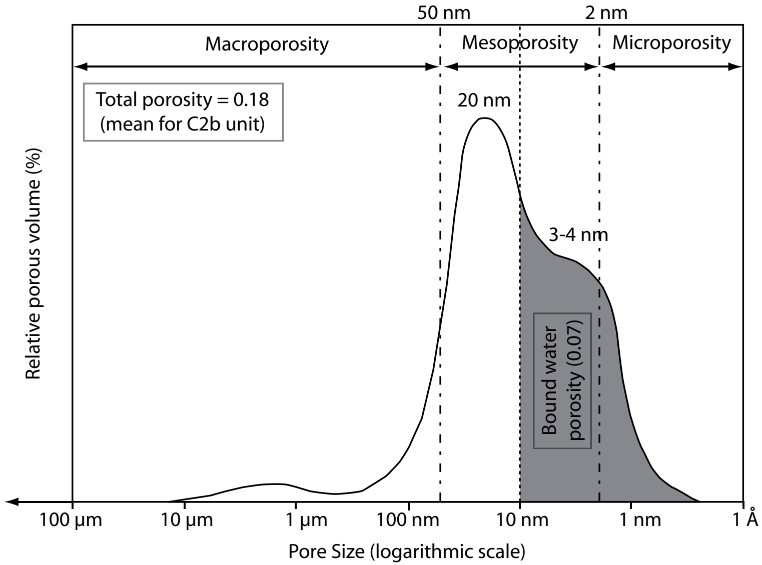

Fig. 2. Conceptual model for pore size distribution in the C2b unit of Callovo-Oxfordian argillites (from ANDRA, 2005).

HESSD

5, 2409–2423, 2008

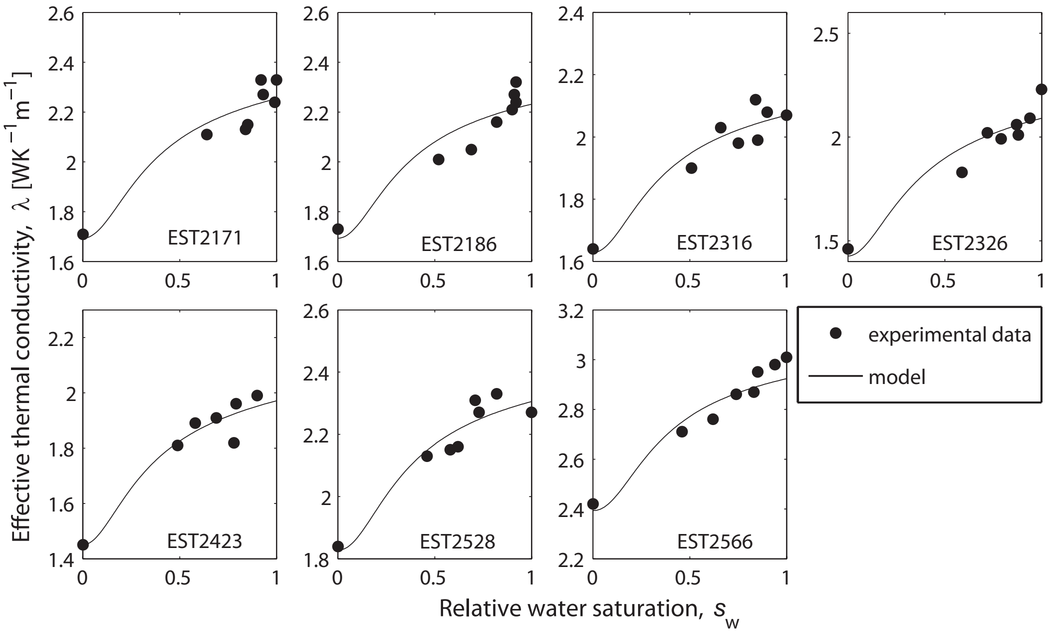

Fig. 3. Optimized model and experimental data comparison for seven samples of COx argillites. Optimized parameter values are located in Table 1.

HESSD

5, 2409–2423, 2008

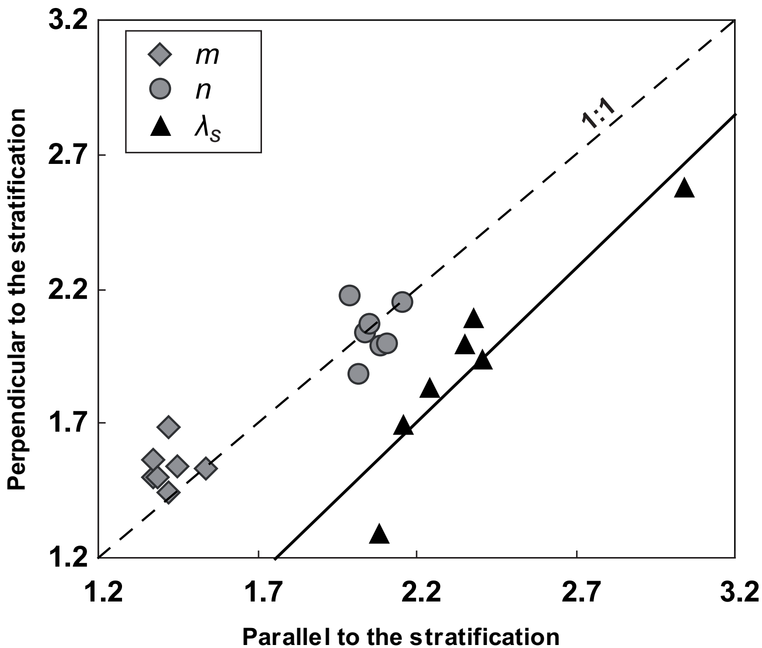

Fig. 4. Comparison between optimized parameters (m, n, and λ_s) with respect of the COx argillite bedding. The plain line presents a linear regression between the two solid phase thermal conductivity optimized from measurements made parallel and perpendicular to the stratification ($\lambda_{s(//)}$ and $\lambda_{s(+)}$,respectively, with $\lambda_{s(//)}=1.14\lambda_{s(+)}-0.81$, $R_N=0.020$).